Advances in Science and Technology Research Journal

Advances in Science and Technology Research Journal 2022, 16(6), 108–117
https://doi.org/10.12913/22998624/155941
ISSN 2299-8624, License CC-BY 4.0

Received: 2022.07.18
Accepted: 2022.11.17
Published: 2022.12.01

Effect of Workpiece Slenderness on the Numerical Flow Lines Distribution in the Cross-Section of a Circular-Symmetric Part Hot Die Forged with a Hammer

Tomasz Miłek[1]

[1] Faculty of Mechatronics and Mechanical Engineering Kielce, University of Technology, Al. Tysiąclecia Państwa Polskiego 7, 25-314 Kielce, Poland

* Corresponding author's e-mail: tmatm@tu.kielce.pl

ABSTRACT

The paper presents the results of computer simulations of the steam-air hammer driven die forging process of circular-symmetrical forgings at different slenderness values of the billet (range from 1.5 to 2.8). The slenderness of the workpiece is defined as the ratio of the length of the billet to its diameter. The aim of investigations was to analyse the influence of various values of the billet upsetting ratios on the distribution of the flow lines in the longitudinal sections of the forgings. In addition, the material flow velocities were compared, which allowed for the evaluation of the flow kinematics in individual zones of the forgings. The computer simulation was performed using specialized commercial QFORM-2D software based on the finite element method (FEM). A comparative analysis of obtained results allowed for the development of conclusions that may be helpful in the implementation of this process in industrial conditions for similar shapes of steel forgings.

Keywords: engineering processes, metal forming, forging, computer modelling, FEM, flow lines

INTRODUCTION

An important stage in the construction of circular-symmetric forgings for hot open die forging utilizing a steam-air hammer is the determination of the dimensions of the workpiece (diameter and length of the billet). The literature guidelines [1–3] suggest that in this case the material diameter should be calculated assuming the maximum allowable slenderness (at which the material does not yet buckle). The slenderness of the workpiece or upsetting factor (s) is defined as the ratio of the length of the billet to its diameter. This factor appears, inter alia, in the formula (1) for determining the diameter of the starting material for a circular-symmetric forging (D_w) [1,3]:

$$D_w = 1.08 \cdot \sqrt[3]{\frac{V_w}{s}} \qquad (1)$$

where: V_w –volume of starting material (mm³),
$s = \frac{L_w}{D_w}$ – slenderness of starting material, for forging using hammer $s = 1.5 \div 2.8$ [1,3],
L_W – the length of the billet; (mm),
D_W – the diameter of the billet, (mm).

Adopting the maximum slenderness allows to obtain a smaller diameter of the material, which reduces the costs of cutting and the heating time. However, in the case of some shapes of circular-symmetric forgings, during forging from a billet with the maximum allowable slenderness, problems may occur with the filling of the die cavity or there may be forging defects such as laps or internal cracks in the material. Subsequently, it may be necessary to analyse the material flow during hot die forging by also using other slenderness values of the workpiece. This situation especially comes about when forging is done using a steam-air hammer, which is a very dynamic process (for example, compared to forging with a crank press).

There was a rapid growth of computing power in the nineties, which significantly facilitated the application of the finite element method (FEM) in computer modelling of forming processes. Since then, numerous continuously improved commercial programs based on this method have been developed. Metal forming, especially associated with forging, uses the following suites, among others: DEFORM, FORGE, MARC Autoforge, ABAQUS, QForm or MSC Superforge [4,5]. They enable simulating forging processes and obtaining results in the field of distribution of effective strain, mean stress, flow stress, temperatures, velocity vectors or, e.g., load force change graphs as a tool displacement function. Although such software enables a detailed analysis of the said results, the forging industry still demands procedures that would allow to provide a quick answer to seemingly simple questions on the possibility of a given forging without forging defects, preferably directly from a rod section or whether the material correctly fills the die impression. Essential aspects in modelling include user's experience and expertise, software proficiency, ability to process input data and their entering time. A computer's computing power is important but of secondary (lesser) significance in relation to the above.

The author reviewed recently published several dozen papers on analysing the analysing the results of hot die forging computer modelling of circular-symmetric forgings, issues arising in the course of their forming and general challenges faced by the forging industry and the development trends appearing therein. Some of them from recent years were selected [4–16]. Gronostajski [4] with his team of peers composed of scientists from several academic centres presented the latest development trends related to numerical and experimental studies of various metal forming processes, including die forging. The study discusses different aspects associated with computer modelling with the use of original, recently developed solutions of the authors. In his last paper, Ghassemali [6] summarized the knowledge in the field of forging and discussed the impact of material behaviour on forming processes. He pointed the main limitations of this process, which include possible oxidation during hot forging, limitations in selecting the material for forging (workability) and related maintenance costs of forging tools. Choi et al. [7] conducted a FEM analysis of the die forging process in relation to the production of circular-symmetric shapes, such as spindles, rotors, etc. They focused on the impact of feed rate and rotation angle on optimal forging pass design. Using FEM, Jayanthi et al. [8] modified the forging process of compressor discs used in aviation engine applications. Their numerical analysis involved load, temperature, strain and material flow behaviour. The analysis constituted a base to recommend a two-stage material upsetting from a cylindrical billet, using a hydraulic press and pneumatic hammer die forging. Similarly, by using the FEM analysis, Zhang et al. [9] introduced changes into the technological process, in this case involving a disc-type steering knuckle used in commercial vehicles. They suggested precision forging instead of a traditionally horizontal open pre-forging and large-flash end forging. The authors demonstrated coherence of the simulation results with the actual process conducted on a program-controlled hammer and CNC electric screw press.

In their paper, Doege and Bohnsack [10] showed different variants of the hot forging of circular-symmetrical forgings, such as straight and helical gears, using a special closing device for forging dies. Keshtiban et al. [11] investigated the production process with closed die forging of one of the most important parts of the gearbox of Mercedes-Benz 10-wheel truck as a case study. They chose this component because of its high operating loads (mechanical and thermal stresses in its working conditions). Based on finite element simulation results in ABAQUS software, they assessed the impact of selected parameters on the forging of the relevant workpiece. Some authors of papers [12–14] tried to identify defects in forgings in selected die forging processes. Hawryluk and Jakubik [12] conducted FEM modelling of a forging defect consisting of the formation of underfills due to air pockets between the forging and the tool. They compared the results of the simulation with the results of the macroscopic, microstructural and defectoscopic examinations. Gao et al. [13], in turn, prepared FEM models for the formation of three types of folding defects. They classified these defects into the following types: confluence-type, bending-type and local-loading type. They proposed a folding index based on the integration of the strain rate over the free surface of the workpiece, which could evaluate the risk of all three typical types of folding. Zheng et al. [14]

investigated the formation mechanism of folding defects for the forging of axisymmetric flanged parts. They described four proposed forming processes for the case-study multi-flanged part. Considering the analysis of the material flow, energy consumption, folding formation, and product precision, they chose the variant for which they carried out experimental tests. The results identified the formation of a small and irregular fold of the material. Interesting results were shown by the authors [15,16] regarding the circular-symmetrical cold forging of billets in the form of segments of the tubes. Winiarski et al. [15] showed the results of a numerical analysis of a cold forging process for a hollow flanged part. The developed process consisted of six stages with the use of methods such as extrusion with a movable sleeve, open-die extrusion, and upsetting. Samołyk [16] showed the results of a numerical analysis (by FEM) of a forging process for producing a hollow ball from a tube made from 19MnCr5 steel. He investigated the impact of the geometric parameters of the billet on the forging process and desired dimensions of the forged workpiece.

The research carried out by the author in this paper is designed to extend the knowledge of computer-aided design for hot die forging of circular-symmetrical forgings regarding the aspects omitted in the available literature dealing with the subject. In the opinion of the author, the general recommendations included in existing literature, which suggest the adoption of maximum workpiece slenderness (s = 2.8) as a rule when calculating its diameter, are insufficient without a discussion of certain reservations. Based on his experience with the design of forging processes (as well as many years of practice since the 1990s with computer simulations of forging processes, hydroforming, solid and backward extrusion, and the pushing process), the author picked an interesting case that was not consistent with the general standards for the relevant design process. During the review of the literature (the results of this review for selected papers [4, 6–16] are shown above), no information has been found about the impact of the selection of geometric parameters of the workpiece on material flow kinematics during forging. The discussed kinematics, in turn, has an impact on the forging process, including, in particular, on the correct filling of the die cavity and the probability of forging defects. The current paper is an attempt at filling the identified gap in the research. It presents the results of computer simulations of the die forging process of circular-symmetrical forgings when a steam-air hammer is utilized and different slenderness values of the billet (range from 1.5 to 2.8) are applied. A wide-flange forging was constructed based on literature guidelines [1, 3] for the machine part manufactured within the industry (shown in Figures 1 and 2, respectively). The aim of investigations was to analyse the influence of various values of the billet upsetting ratios on the distribution of the flow lines in the longitudinal sections of the forgings. In addition, the material flow velocity was compared, which allowed for the evaluation of the flow kinematics in individual zones of the forgings.

MATERIAL FLOW FORMULATION AND ASSUMPTIONS IN SIMULATION

The computer simulation was performed using specialized commercial QFORM-2D software based on the finite element method. It is intended for modelling primarily forging and extrusion processes, and the successive results are reliable [17, 18]. The forged material was considered to be an incompressible rigid-plastic continuum and elastic deformations were neglected. The system of governing equations included the following [17]:

- equilibrium equations

$$\sigma_{ij,j} = 0 \tag{2}$$

- compatibility conditions

$$\dot{\varepsilon}_{ij} = \frac{1}{2}(v_{i,j} + v_{j,i}) \tag{3}$$

- constitutive equations

$$\sigma'_{ij} = \frac{2\bar{\sigma}}{3\dot{\bar{\varepsilon}}}\dot{\varepsilon}_{ij} \tag{4}$$

- incompressibility equation

$$v_{i,i} = 0 \tag{5}$$

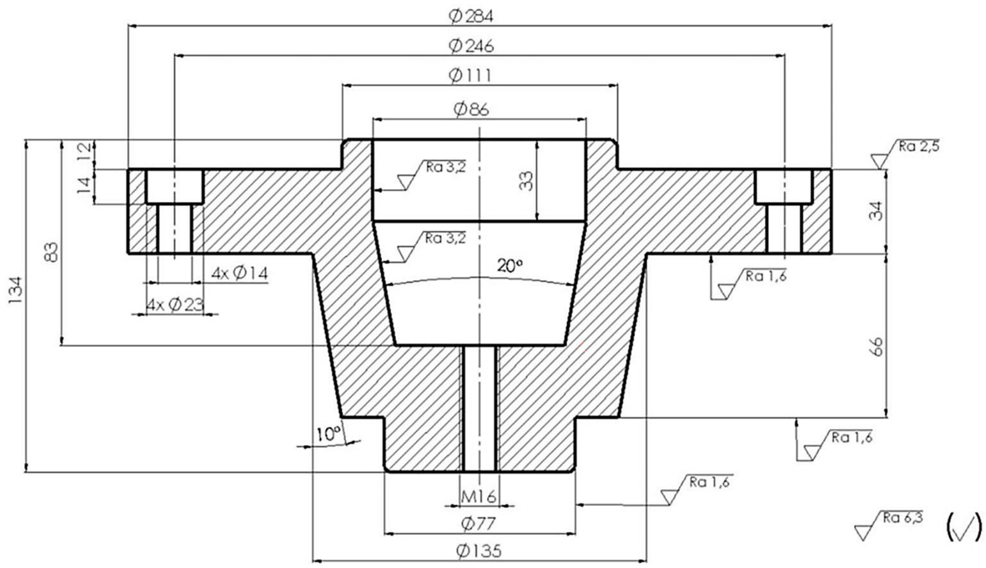

Figure 1. Drawing of the circular-symmetric element made from C22 steel

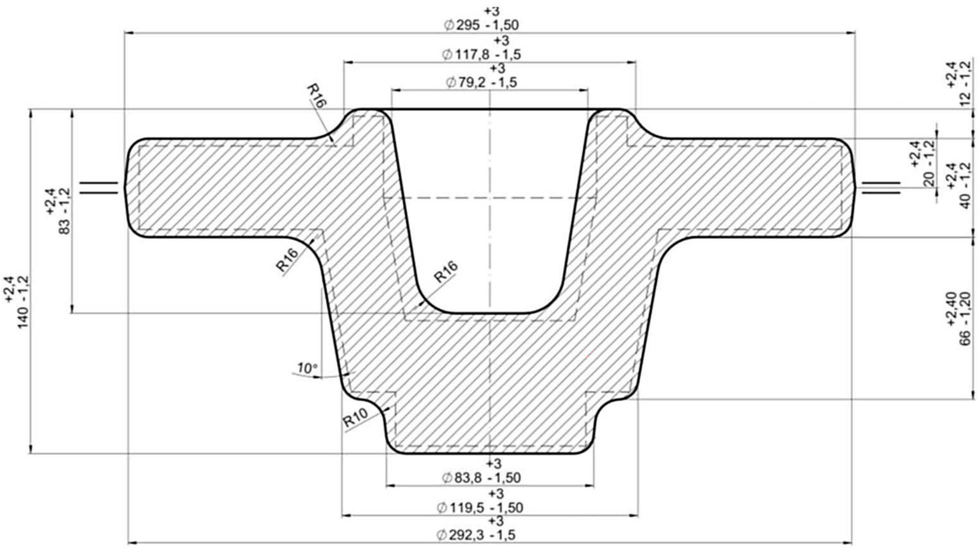

Figure 2. Drawing of the circular-symmetric hammer forging forged in the regular accuracy class, where: outer and inner drafts are 6° and 9°, respectively; non-dimensioned fillet radii r = 8 mm; permissible joggle is 1.4 mm; flash residue is 1.7 mm.

- expression for flow stress

$$\bar{\sigma} = \bar{\sigma}(\bar{\varepsilon}, \dot{\bar{\varepsilon}}, T) \tag{6}$$

where: σ_{ij} and $\dot{\varepsilon}_{ij}$ – components of stress and strain-rate tensors,
v_i, – velocity components,
σ_{ij}' – deviatoric stress tensor,
$\bar{\sigma}, \bar{\varepsilon}, \dot{\bar{\varepsilon}}$ – effective stress, strain and strain-rate, respectively,
T – temperature.

In Eqs 2–6, the summation convention was applied. The prime denotes a derivative with respect to the axis following it. The indexes *i* and *j* for two-dimensional problems vary from *1* to *2*, and repeated subscript represents summation. The friction model proposed by Levanov et al. [17] was used for the contact region of workpiece surface. Equation (7) can be considered as a combination of the constant friction model and the Coulomb friction model. The formula combines the advantages of both models [17]:

$$F_t = m\frac{\overline{\sigma}}{3}(1-\exp(-1.25\frac{\sigma_n}{\overline{\sigma}}) \quad (7)$$

where: m – the friction factor,
σ_n – the normal contact pressure.

The charge material in the form of C22 steel rod sections of various dimensions specified in Table 1 was used in the simulation. The values of the diameters of the starting material D_0 were taken from the production programme for steel industries on the basis of the calculated diameters D_w from the formula (1). The billet lengths L_w used in the simulation were calculated from the constant volume condition for D_0.The material was chosen from the available software database. Its flow stress was dependent on strain, strain rate and temperature.

Forging charge heating temperature was 1100 °C. The flash land thickness was assumed at 4 mm, which corresponded to the final minimum distance between the tools. It resulted from the adopted type and dimensions of the flash gap. The flash gap with a one-sided magazine made in the upper die was used in the simulations because it is recommended for most of the forgings with circular-symmetrical shapes [1–3]. For modelling purposes, it was modified by opening the magazine as recommended in [19]. The shape and dimensions before and after modification are shown in the Figures 3 and 4, respectively.

Between the die impression, and the top and bottom material surface the simulation assumed using grease intended for hot forging of steel forgings with a friction factor m=0.4 and a heat transfer coefficient of 3000 W/(m^2 K), as recommended in [19]. The ambient temperature for a process conducted under actual conditions was set at 20 °C. In turn, actual material exposure times were assumed at: 5s for transferring a material after heating from the furnace to the dies and 5s for a material placed on the bottom die before deformation. An air-steam hammer with an impact total energy of 250 kJ and equal top and bottoms dies of 119 tons was selected for forging.

RESULTS AND ANALYSIS

The study involved conducting a number of computer simulations of the hot die forging process (shown in Figure 2) using charge materials (dimensions from Table 1) and the air-steam hammer, and other boundary conditions discussed in chapter 2. The longitudinal forging sections were plotted on a Lagrange mesh in order to analyse material flow and deformation (a system of 10 horizontal and 10 vertical lines was determined) during forging. The results obtained for slenderness values of s = 1.5, s=1.9; s=2.4 and s=2.8, respectively, are shown in Figure 5. In addition, Figure 6 shows the designation of characteristic zones within the material cross-section during deformation, on the example of a forging obtained from a pre-from with a slenderness of s=1.5. Laps appeared when forging forgings using pre-forms with extreme slenderness values (minimum and maximum) of s=1.5 and s=2.8, respectively. While, in the case of forging using charge with s=1.5, the forging began to form at the 8th simulation stage (Figure 5a) in the forging *D* zone (as per the zone designation in Figure 6). A forging defect was found in the outer part of the forging flange due to obstructed radial flow of the material. In turn, in the case of forging using a preform with s=2.8, a lap appeared at the 6th simulation stage (Figure 5d), in the forging *B* zone. In this case, the forging defect began forming on the internal surface of the forging blind hole, due to material upsetting in this zone.

As dictated by the standard approach found in source literature [1–3], eliminating the probability of forging defects appearing in the discussed

Table 1. Dimensions of billets used in the modelling

Values of slenderness s for calculating D_w from formula (1)	Values of diameters D_w from formula (1) (mm)	Values of diameters of starting material used in simulations D_0 (mm)	Values of length L_w of starting material used in simulations (mm)
1.50	148.1	150	219
1.90	136.9	140	251
2.15	131.3	135	270
2.40	126.6	130	291
2.80	120.3	120	342

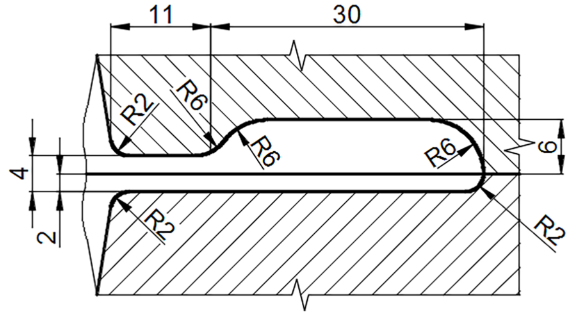

Figure 3. Shape and dimensions of the flash gap with a flash land and a magazine for die forging of circular-symmetrical forgings with the hammer

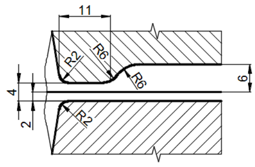

Figure 4. Modified shape of flash gap for simulation of die forging

zones, when using forgings with *s*=1.5 as well as *s*=2.8, would require modifying the die impression through increasing forging inclinations and rounding radii, in the *D* and *B* forging zones, respectively. Based on the conducted simulations, it turned out that there was also another solution to this issue. Modelling the process of forging using a material with slenderness *s* = 1.9–2.4 no longer exhibited the probability of laps in forging B and D zones (as shown in Figures 5b and 5c, respectively). Material flow kinetics within the discussed zone improved significantly. This fact was additionally confirmed by simulations conducted for a case of a forging from a preform with a slenderness of s=2.15 (a-i stages in Figure 7). The material correctly filled the die cavity in B zone during stage 5 of the simulation (Fig. 7e) and in D zone and the bottom part of the die cavity during stage 7 (Fig. 7g). The final forging made at the last stage (Fig. 7i) did not show the probability of any forging defects.

In addition, Figure 8 shows the distribution of material flow velocity vectors within the longitudinal sections of forgings made of preforms with a slenderness of s=1.9 and s=2.4, for which the forging process produced no defects. When analysing them, one can conclude that the most intensive radial material flow in the forging flange section can be observed when using a starting material with s=2.4, compared to forming using a material with s=1.9. In addition, the material filled the die impression in the lower part of the forging quicker and easier, which is understandable in the light of the lower charge material diameter (similar to the lower die part impression diameter).

The comparison of stage 3 of the simulation for forgings from workpieces with slenderness values s = 1.9 and s = 2.4 (Figs. 8a and 8b, accordingly) indicates that the material in the latter case not only shows more intensive radial flow in D zone (outer flange of the forging) but also more quickly fills the area in B zone – the internal surface of the blind hole of the forging. At stage 5 of the simulation, the material forged from the workpiece with s = 2.4 (Fig. 8b) has already filled the die cavity in D zone (forging flange), whereas with s = 1.9 in the same zone (Fig. 8a), a part of the die cavity remained unfilled. It was filled during the following stage (stage 6) of the simulation (Fig. 8a).

Considering the results of the conducted simulations of the forging of workpieces with the individual slenderness values (s = 1.5, s = 1.9, s = 2.15, s = 2.4, s = 2.8), it was observed that, along with the increase in slenderness, the material had more difficulty with filling the die cavity in B zone (inside of the blind hole), resulting in a forging defect in that area for the maximum slenderness s = 2.8. Irrespective of the adopted slenderness of the forging workpieces, the material eventually correctly filled the die cavity in A zone (bottom of the blind hole) and C zone (flash forming area), respectively. In D zone (external area of the flanged part of the forging), there were problems with the filling of the die cavity, beginning at stage 7 of the simulation (Fig. 5a), which resulted in the formation of a forging defect at stage 8 for the forging made from the workpiece with s = 1.5. The best results in terms of the correct filling of the die cavity and material flow intensity were achieved for forgings from workpieces with slenderness values s = 1.9, s = 2.15 and s = 2.4.

The last stages of modelling hot die forging for various coefficients *s* which are shown in Figure 3 (for s = 1.5; s = 1.9; s = 2.4; s = 2.8, respectively) and in Figure 5 (for s = 2.15) and in Figure 6 (for s = 1.9 and s = 2.4) differ in the size of the flash. For the forgings that did not show the probability of forging defects (i.e. for s = 1.9; s = 2.15 and s = 2.4), the flash land thickness was 4 mm (i.e. according to the assumed simulation boundary conditions). On the other hand, in the case of forgings with the coefficients s = 1.5 and s = 2.8, in

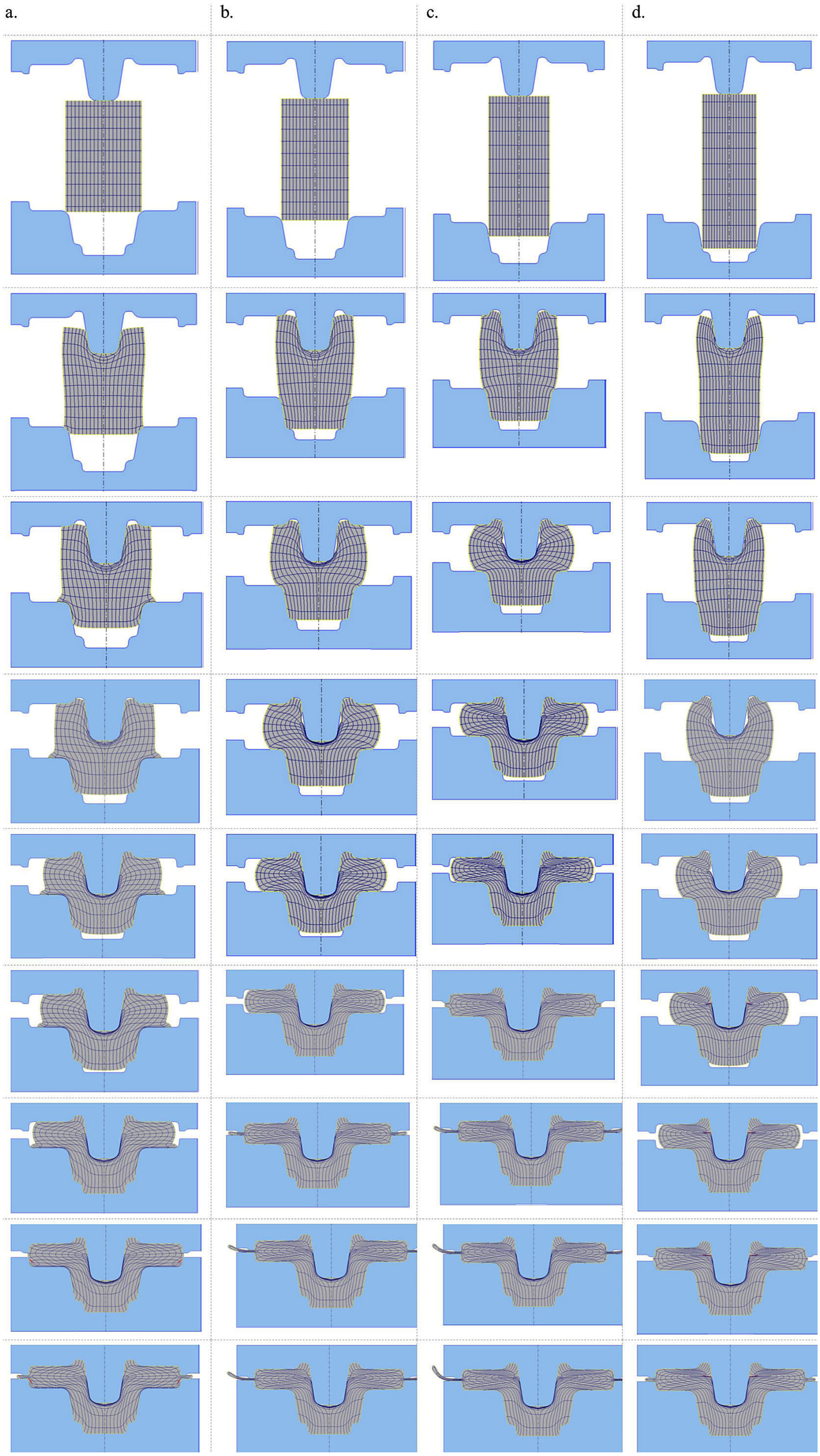

Figure 5. Numerically computed stages of the hot die forging process (with flow lines distributions) for various billet slenderness: a. s = 1.5; b. s = 1.9; c. s = 2.4; d. s = 2.8

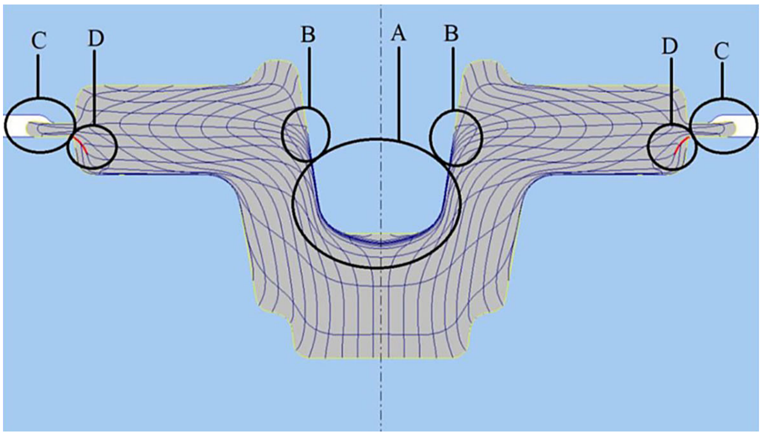

Figure 6. Determination of characteristic zones in the cross-section of a forging obtained from a preform with a slenderness of s = 1.5

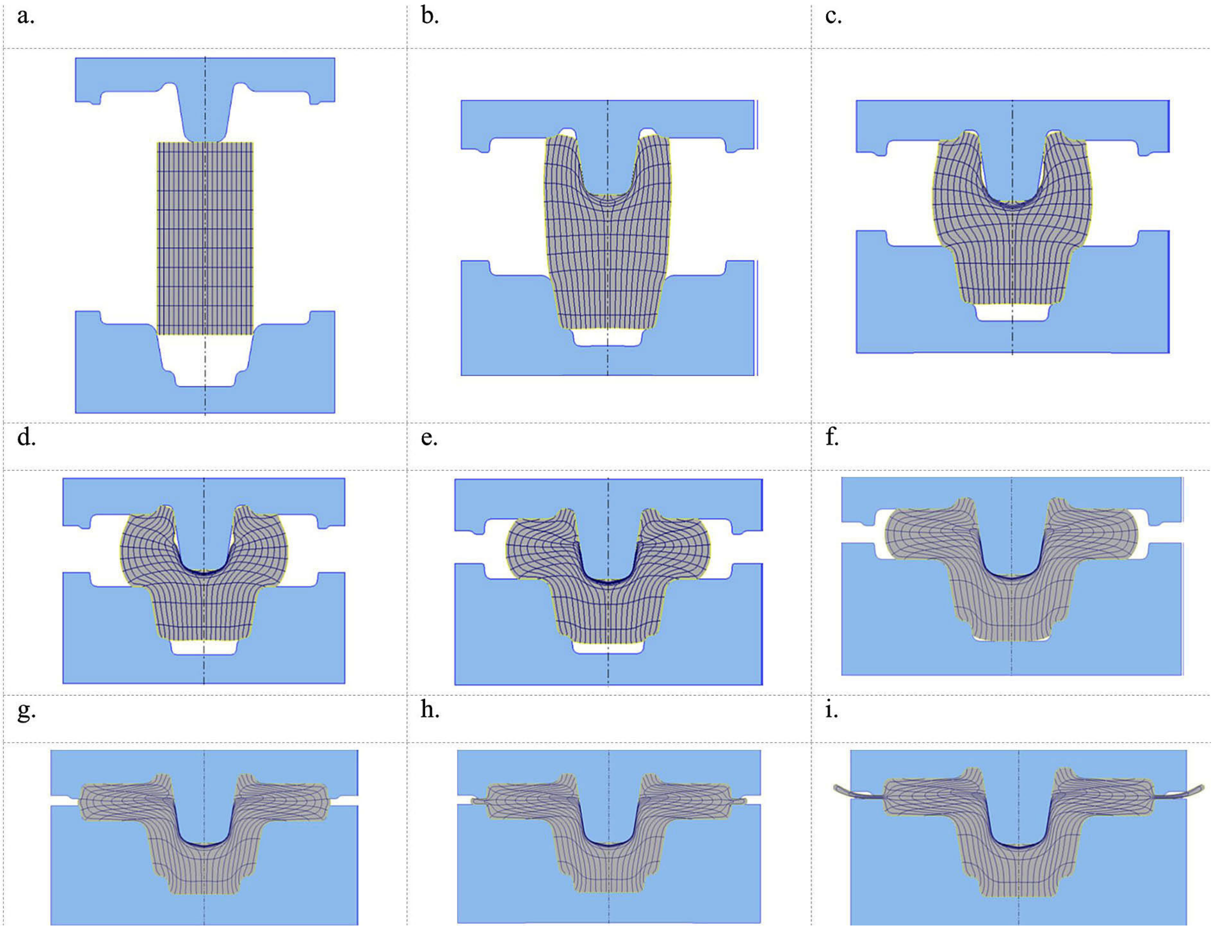

Figure 7. Stages (a. – i.) of the hot die forging process (with flow lines distributions) obtained when simulating billet slenderness s = 2.15

the modelling of which defects were found, it was not possible to obtain the assumed the flash land thickness. In these variants, the thicknesses obtained in the last steps were 6.5 mm and 6.8 mm, respectively. This resulted in a significantly smaller amount of flash compared to the variants of forgings for s = 1.9; s = 2.15 and s = 2.4.

CONCLUSIONS

Although the obtain test result may be treated as a certain case study, when developing an air-steam hammer hot die forging technology for steel forgings of specific shapes, namely, circular-symmetric with a wide flange, it is possible to use them to a greater extent in order to avoid the

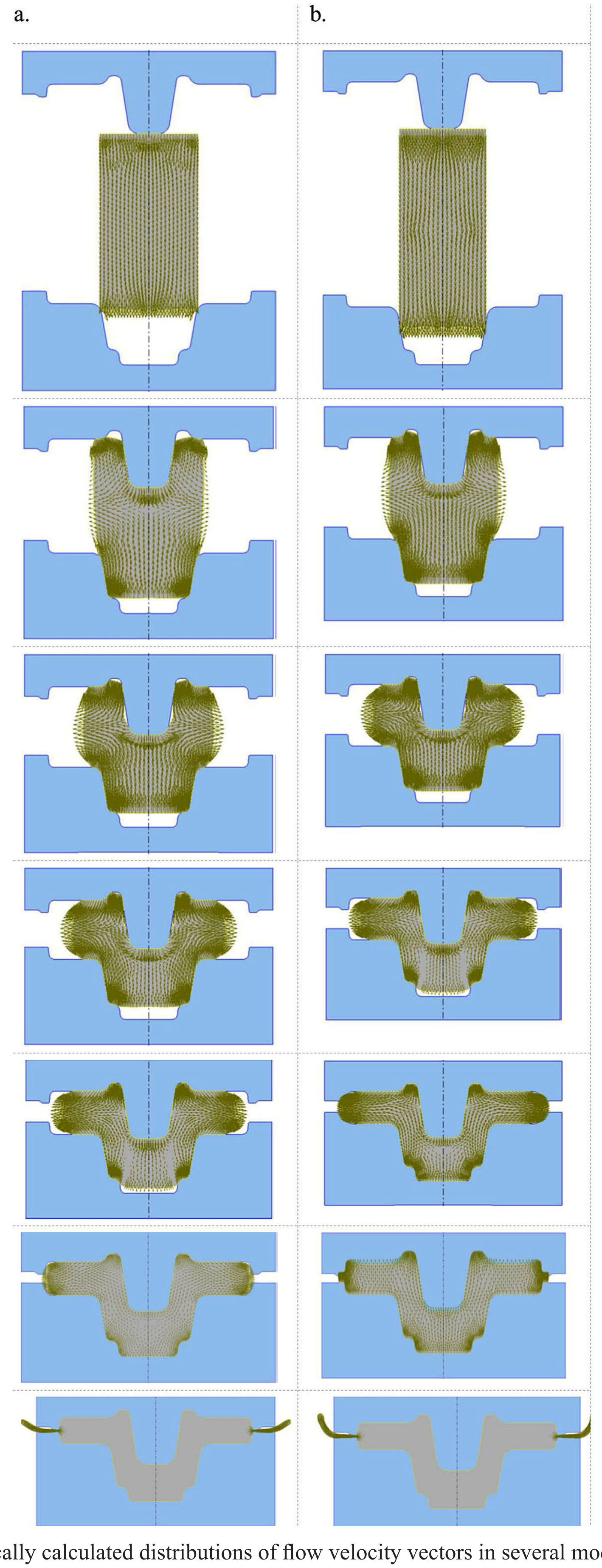

Figure 8. Numerically calculated distributions of flow velocity vectors in several modelling stages at the intersections of hot die forged forgings for selected billet slenderness: (a) s = 1.9 and (b) s = 2.4; respectively

probability of forging defects within the manufacturing process that results from the selection of specific charge slenderness values. The presented results were obtained only within modelling with software based on FEM and were not verified experimentally. Despite this fact and generally known shortcomings of the FEM method, they can be deemed reliable, since the discussed method is still recognized as the most perfect tool for simulating plastic forming processes, including hot die forging, provided that the boundary conditions are specified precisely.

On the basis of the computer modelling of the hot die forging process of a circular symmetrical part, it was found that the assumption of extreme permissible slenderness of billets (i.e. s = 1.5 and s = 2.8) for forging has a relatively high probability of forging defects which may occur at the outer part of the forging flange in first case, and in the internal surface of the forging blind hole in the second case. Therefore, it is recommended to use the intermediate values of slenderness of the workpieces for the same forgings or similar shapes, i.e. from s = 1.9 to s = 2.4 for which the probability of forging defects in computer modelling did not occur.

REFERENCES

1. Wasiunyk P. Die forging. WNT, 1987 (in Polish).
2. Lange K. Handbook of metal forming. McGraw-Hill Book Company, 1985.
3. Pacanowski J. Design principles for die forging of circular-symmetric forgings. Kielce University of Technology, 2021 (in Polish).
4. Gronostajski Z., Pater Z., Madej L., Gontarz A., Lisiecki L., Łukaszek-Sołek A., Łuksza J., Mróz S., Muskalski Z., Muzykiewicz W., Pietrzyk M., Śliwa R. E. Tomczak, J. Wiewiórowska S., Winiarski G., Zasadziński J.,Ziółkiewicz S. Recent development trends in metal forming. Archives of Civil and Mechanical Engineering 2019, 19(3): 898–941.
5. Kocańda A. Selected directions of development of metal forming. Przeglad Mechaniczny 2000, 3: 6–11.
6. Ghassemali E. Forging of Metallic Parts and Structures. Encyclopedia of Materials: Metals and Alloys 2022, 4: 129–143.
7. Choi S.K., Chun M.S., Van Tyne C.J., Moona Y.H. Optimization of open die forging of round shapes using FEM analysis. Journal of Materials Processing Technology 2006, 172(1): 88–95.
8. Jayanthi A., Anilkumar M., Ravisankar B. Selection of forging process for compressor disc for aero engine using finite element analysis. Materials Today: Proceedings 2022, 60: 2111–2116.
9. Zhang Y., Huang S.C.M., Deng Y.Y.O., Li S., Xia J., Deng L., Jin J. Research and application of precision forging forming process for flat thin flash of automobile disc steering knuckle. Procedia Manufacturing 2020, 50: 32–36.
10. Doege E., Bohnsack R. Closed die technologies for hot forging. Journal of Materials Processing Technology 2000, 98(2): 165–170.
11. Keshtiban P.M., Taher A., Keshtiban M.M. Practical study and finite element simulation of production process of the bush of gearbox of Mercedes-Benz 10-wheel truck by closed die forging. Journal of Computational Applied Mechanics 2021, 52(1): 69–84.
12. Hawryluk M., Jakubik J. Analysis of forging defects for selected industrial die forging processes. Engineering Failure Analysis 2016, 59: 369–409.
13. Gao P.F., Fei M.Y., Yan X.G., Wang S.B., Li Y.K., Xing L., Wei K., Zhan M., Zhou Z.T., Keyim Z. Prediction of the folding defect in die forging: A versatile approach for three typical types of folding defects 2019, 39: 181–191.
14. Zheng J.-Y., Fang J.Y.C., Fu M.W. Flow-induced folding in multi-scaled bulk forming of axisymmetric flanged parts and its prediction and avoidance 2022, 119: 5863–5883.
15. Winiarski G., Bulzak T.A., Wójcik Ł., Szala M. Numerical analysis of a six stage forging process for producing hollow flanged parts from tubular blanks. Advances in Science and Technology Research Journal 2020, 14(1): 201–208.
16. Samołyk G. Numerical analysis of a forging process for producing a hollow ball from tube. Advances in Science and Technology Research Journal 2018, 12(3): 150–157.
17. Biba N., Stebunov S., Vlasov A. Material forming simulation environment based on QFORM3D software system. Steel Research International 2008, 79: 611–616
18. Miłek T., Kowalik B., Kuliński B. Evaluation of the possibility of performing cold backward extrusion of axisymmetric thin-walled aluminium die stampings with square section. Archives of Metallurgy and Materials 2015, 60(4): 3043–3049.
19. QFORM 2D/3D. Metal forming simulation program. 2D simulation User's Guide. QuantorForm Ltd. 2008